Souma Chowdhury
Research Assistant Professor
Member of ASME
Multidisciplinary Design
and Optimization Laboratory (MDOL),
Department of Mechanical
and Aerospace Engineering,
Syracuse University,
Syracuse, NY 13244
e-mail: sochowdh@syr.edu

Jie Zhang
Post Doctoral Research Associate
Member of ASME
Multidisciplinary Design
and Optimization Laboratory (MDOL),
Department of Mechanical
and Aerospace Engineering,
Syracuse University,
Syracuse, NY 13244
e-mail: jzhang56@syr.edu

Weiyang Tong
Multidisciplinary Design
and Optimization Laboratory (MDOL),
Department of Mechanical
and Aerospace Engineering,
Syracuse University,
Syracuse, NY 13244
e-mail: wtong@syr.edu

Achille Messac[1]
Dean of the Bagley College of Engineering
Professor and Earnest W.
and Mary Ann Deavenport, Jr. Chair
Fellow of ASME
Aerospace Engineering,
Mississippi State University,
Mississippi State, MS 39762
e-mail: messac@bagley.msstate.edu

Modeling the Influence of Land-Shape on the Energy Production Potential of a Wind Farm Site

During wind farm planning, the farm layout or turbine arrangement is generally optimized to minimize the wake losses, and thereby maximize the energy production. However, the scope of layout design itself depends on the specified farm land-shape, where the latter is conventionally not considered a part of the wind farm decision-making process. Instead, a presumed land-shape is generally used during the layout design process, likely leading to sub-optimal wind farm planning. In this paper, we develop a novel framework to explore how the farm land-shape influences the output potential of a site, under a given wind resource variation. Farm land-shapes are defined in terms of their aspect ratio and directional orientation, assuming a rectangular configuration. Simultaneous optimizations of the turbine selection and placement are performed to maximize the energy production capacity, for a set of sample land-shapes with fixed land area. The maximum farm capacity factor or farm output potential is then represented as a function of the land aspect ratio and land orientation, using quadratic and Kriging response surfaces. This framework is applied to design a 25 MW wind farm at a North Dakota site that experiences multiple dominant wind directions. An appreciable 5% difference in capacity factor is observed between the best and the worst sample farm land-shapes at this wind site. It is observed that among the 50 sample land-shapes, higher energy production is accomplished by the farm lands that have aspect ratios significantly greater than one, and are oriented lengthwise roughly along the dominant wind direction axis. Subsequent optimization of the land-shape using the Kriging response surface further corroborates this observation. [DOI: 10.1115/1.4026201]

Keywords: capacity factor, farm land-shape, response surface, wind distribution, wind farm layout optimization

1 Introduction

1.1 Wind Farm Planning. The steady evolution of renewable energy technologies is necessary to drive the world towards a more sustainable and environment-friendly energy demographics [1,2]. Wind power plants or wind farms lie at the forefront of such renewable energy technologies. The energy output and the economics of a wind farm are functions of a series of environmental and engineering factors. Optimal choice/design of the engineering factors depends on the estimated wind resource variations and other natural characteristics of the site and its surroundings. These relationships are generally not independent of each other. Therefore, for a given site, the overall wind farm configuration should be carefully planned in order to accomplish the desired level of performance. On the contrary, in conventional wind farm development, decision-making regarding the major engineering factors are often performed individually. Overlooking the interaction among the engineering factors can lead to suboptimal planning of the wind farm configuration.

Key engineering-design factors that influence the wind farm performance include:

(1) the nameplate capacity of the wind farm
(2) the land area and land-shape of the farm site
(3) the type(s) of turbine to be installed
(4) the placement of turbines in the wind farm (farm layout)

A coherent consideration of the influences of the different key design factors on wind farm performance is rare in the literature. For example, turbine choices are often proposed based on the estimated class of wind power density and wind loads for the concerned site. Such information pertains to each turbine operating as a standalone entity; the performances of the turbines as part of an array, which is highly sensitive to the mutual wind-shading effects, often remains unaccounted for. Another instance of neglecting *factor-interdependence* occurs during farm layout planning; designing the arrangement of turbines in the farm is conventionally performed as an independent post-process to planning the "nameplate capacity" and the "portion of the site to be used for wind turbine installation." The latter factor can be more readily represented as farm land-shape and farm land area. For the same installed capacity and overall land area used for wind farm

[1]Corresponding author.

Contributed by the Advanced Energy Systems Division of ASME for publication in the JOURNAL OF ENERGY RESOURCES TECHNOLOGY. Manuscript received March 26, 2013; final manuscript received November 22, 2013; published online February 28, 2014. Editor: Hameed Metghalchi.

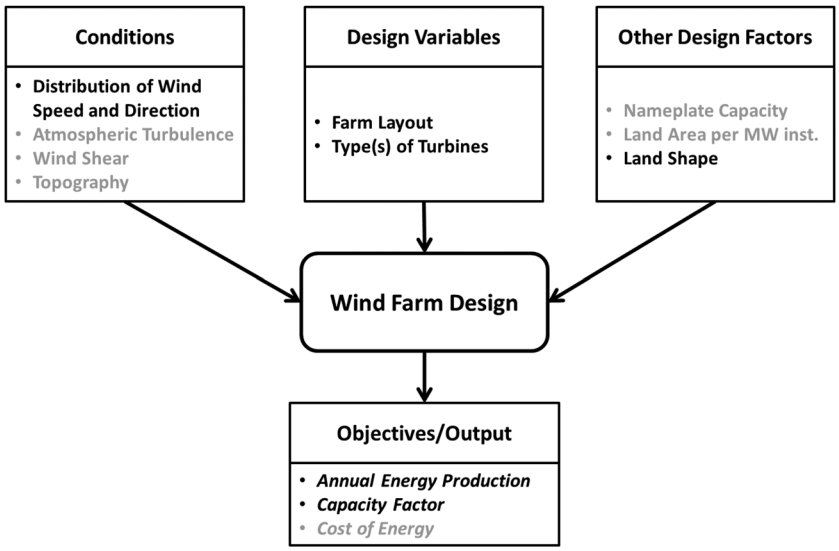

Fig. 1 Key factors (inputs and outputs) in wind farm design

construction, different farm land-shapes can have significantly different energy production capacities. In other words, the farm land-shape strongly regulates the maximum energy that can be accomplished through layout optimization. Investigation into such scenarios is rare in the literature.

The key inputs and the outputs of a generalized wind farm design methodology are illustrated in Fig. 1. The input and the output parameters of wind farm design that are considered in this paper appear in black font in Fig. 1; the parameters/factors that have not been explicitly considered or are assumed to be constant appear in gray font. The focus of this paper is on the role of the farm land-shape in optimal wind farm design.

The specific objectives of this paper are:

(i) To develop a methodology to quantify the relationships between the farm land-shape and the maximum farm performance that can be accomplished through layout optimization.
(ii) To illustrate these relationships and explore their significance in commercial-scale wind farm design.
(iii) To optimize the farm land-shape (for maximizing energy production) using the estimated function defining the "*farm land-shape—farm performance*" relationship.

The first objective essentially leads to the quantification of the energy production potential of a particular land-shape at a given site. In this context, rectangular farm land configurations are considered. Rectangular wind farm land is used to investigate and characterize how wind farm performance is influenced by the aspect ratio and the orientation (i.e., overall shape) of the farm land. Response surface methodologies are used to model the relationships between the land shape and the optimal farm performance.

1.2 Wind Farm Layout Optimization. Wind farms generally consist of multiple wind turbines located in a particular arrangement over a substantial stretch of land (onshore) or water body (offshore). It has been shown that the total power extracted by a wind farm is significantly less than the simple product of the power extracted by a standalone turbine and the number of identical turbines (N) in the farm [3]. This deficiency can be in part attributed to the loss in the availability of energy due to wake effects, i.e., the shading effect of a wind turbine on other wind turbines downstream from it [4]. Energy deficit due to mutual shading effects can be determined using analytical or numerical wake models. These wake models provide a measure of the growth of the wake and the velocity deficit in the wake as functions of the distance downstream from a given wind turbine. The Park wake model, originally developed by Jensen [5] and later by Katic et al. [6], is one of the most popular analytical wake models used in wind farm modeling. Other standard analytical wake models include Frandsen's model [7], Larsen's model [8], and Ishihara's model [9].

The reduction in the wind farm efficiency (loss in the effective energy available), due to this mutual shading, depends primarily on the geometric arrangement of wind turbines in a farm. To address this wake-induced energy deficiency, the arrangement of turbines over the farm site is optimized. Two primary classes of turbine arrangement (or layout optimization) methods exist in the literature: (i) methods that divide the wind farm into a discrete grid in order to search for the optimum grid locations of turbines [4,10–12], (ii) more recent methods that define the turbine location co-ordinates as continuous variables, thereby allowing turbines to take up any feasible location within the farm [13–15]. Other recent methods consider the demand pattern for micro-siting, instead of merely maximizing the net energy production [16]. Various classes of algorithms have also been leveraged for optimizing wind farm layouts, including evolutionary and genetic algorithms [10–12], swarm-based algorithms [15], and pattern search algorithms [17]. However, only a few of the above methods allow optimal selection of commercial turbines along with optimal turbine arrangement [15]. Mustakerov and Borissova [18] presented an optimization methodology to select the type and the number of turbines in a wind farm, where two different wind farm land shapes (square and rectangle) were considered. Gu and Wang [19] presented a method to model irregular farm boundaries, where these irregular shapes were reported to be motivated by factors such as lakes, parks, or ecologically sensitive areas at or near the site.

A limited set of choices of wind turbines (turbine-types) are available in the commercial market. The selection of an optimal combination of turbines from this set yields a mixed-discrete optimization problem. Commercial wind farms often comprise a large number of turbines (a hundred or more); for a wind farm with N turbines, if an array layout or a grid-based pattern is not assumed, the optimization problem is characterized by at least $2N$ design variables. Together with the likely multimodal nature of the power generation function [20], this characteristic leads to a challenging optimization problem. The grid-based approach results in an even higher dimensional integer programming problem. Therefore, in the case of both class of farm layout optimization approaches, powerful optimization methodologies need to be leveraged.

The Unrestricted Wind Farm Layout Optimization (UWFLO) methodology, introduced by Chowdhury et al. [14,15], avoids the limiting assumptions presented by other methods, regarding the layout pattern and the selection of turbines. The original UWFLO power generation model [14] was successfully validated against data from a wind tunnel experiment on a scaled down wind farm. This method was further advanced by Chowdhury et al. [15] to include (i) the variation in wind conditions and (ii) the use of commercial wind turbines. The UWFLO method also allows a combination of differing turbine-types, in order to favorably modify the flow pattern within the farm (for maximum energy production). A powerful mixed-discrete Particle Swarm Optimization (MDPSO) algorithm [21] is used for solving the optimization problems in the UWFLO framework. In this paper, we use the UWFLO method to determine the optimum wind farm configuration for any given farm land-shape.

1.3 Role of Farm Land-Shape in Wind Farm Planning. The optimal farm layout(s) and the corresponding maximum energy production that can be obtained for a wind resource depend on the given/specified boundaries of the farm site. Farm sites generally stretch over a substantial area, and the boundaries to which turbine installations will be constrained are themselves subject to planning and need not be fixed. The maximum energy that can be extracted from a certain farm land-shape (defined by specific boundaries) can be significantly different from that extracted from a different farm land-shape; in other words, the *energy production potential* or *farm output potential* is strongly related to the allowed farm boundaries (farm land-shape). To the best of the authors' knowledge, a wind farm design methodology that explicitly accounts for farm land-shape options and/or explores the relationship between the farm output potential and the farm land-shape is currently lacking in the literature.

A change in the land-shape (allowed boundaries) alters the entire coordinate system defining the farm layout, making it intractable to optimize the farm layout and the land-shape together. Hence, we believe that it is more tractable to develop a bi-level optimization framework for optimizing the farm layout and the farm land-shape. At the same time, the available land at a site is often subject to various other practical constraints owing to (i) local vegetation (and/or land usage), (ii) construction of roadways, (iii) local topography, (iv) load bearing capacity of the soil, (v) negotiations with local land-owners [22], and (vi) spatial variation of the wind resource [23]. A simpler incorporation of these factors as constraints is possible with a bi-level optimization framework. The bi-level optimization framework would also allow investigation of the relationship between the farm land-shape and the corresponding maximum farm performance (obtained through layout optimization), which can provide unique insights into the role of farm land-shape in wind farm design. It is important to note that depending upon the farm layout, different levels of energy production can be accomplished from a particular land-shape (at a site). Hence, the *maximum* energy production capacity or farm output *potential* of a given land-shape is of interest in this context.

The likely impact of the wind farm on its natural surroundings and local neighborhood also depends on the extent of the site used or the land footprint of the wind farm. Land usage for turbine installation generally demands (i) negotiations with local land-owners [22], (ii) consideration of noise and visual impact, (iii) displacement of local wildlife [24], and (iv) reduction or suspension of alternative land usage (e.g., for agriculture or cattle grazing). A standard wind farm site could offer several joined/disconnected plots, belonging either to local land-owners (individuals/organizations) or to the Government. However, using different sets of land plots at the site could offer differing trade-offs with respect to the following objectives: (i) energy production and (ii) ease of land acquisition, and (iii) the net impact on surroundings. These objectives ultimately bear important cost implications. For example, the portion and the extent of the site to be used for wind turbine installation affects the site permitting and land acquisition processes. These processes are known to be potential contributing factors to costly delays in wind energy projects [25].

Hence, it is important to understand how land area and land-shape impact these objectives. Scenarios to be explored could include examples such as—using a different land-shape with the same total area could produce more energy while resulting in acceptable levels of impact on the local surroundings. Exploration of such scenarios requires quantitative frameworks that relate land exploitation (area and shape) to energy production capacity and impact on surroundings. With the availability of such a framework, developers would not need to be restricted to use a predefined portion of the site to fulfill their conceived capacity plans. Such a framework could therefore enable more effective due diligence in the feasibility study stage of wind farm planning.

Very limited amount of research has been done in the wind energy community on quantitatively exploring farm-land availability and options at a site, and their impact on the energy production potential. Christie and Bradley [26] present an otherwise rare exploration of how to optimize land use for wind farms; their paper focuses on maximizing power generation per unit land area. The effects of number of turbines (array size), turbine separation, and perimeter setback are particularly explored in that paper [26]. Christie and Bradley [26] found that wind farms designed to maximize power generation per unit area of land could be significantly different from that designed to maximize economic gain or overall capacity factor. Chowdhury et al. investigated how the installed capacity and the "land area/MW installed" leveraged for a project impacts the optimal energy production capacity of a site [27]. Chowdhury et al. [27] found that in order to ensure a desirable threshold capacity factor, the "*land area—nameplate capacity*" combination should be beyond a particular cutoff curve (which is subjective to the local wind conditions).

In this paper, we develop response surface-based models (or surrogate models) to represent the maximum energy production obtained by farm layout optimization as a function of the farm land-shape. This process also provides key insights into the correlation between the land-shape and the corresponding optimized layout (that maximizes energy production). Subsequently, we again maximize the capacity factor (using the response surface) by optimizing the land-shape. This research is expected to lay the foundation of qualitatively exploring the impact of the site configuration on different production, economic, and environmental objectives in a wind energy project. For example, the novel response surface-based framework developed in this paper could be readily extended to explore how different land-shapes (with implicitly optimized layout) could result in different levels of noise impact or impact on local wildlife. Section 2 describes the overall framework developed to relate the maximum farm energy production capacity to the farm land-shape. Section 3 shows the results from the application of the design framework to a case study, the response surfaces developed thereof, and the maximum capacity factor obtained by optimizing the land-shape.

2 Modeling the Role of Land Aspect Ratio and Orientation in Wind Farm Planning

2.1 Overview of the Modeling Framework. This paper focuses on modeling how the optimal wind farm performance (energy production potential) is influenced by the shape of the farm land. Rectangular farm configurations are considered for the ease of analysis and illustration, and the shape of the farm land is characterized in terms of the *aspect ratio* and the *orientation* of the farm. The aspect ratio of the farm is the ratio of the length to the breadth of the farm land. The orientation of the farm land is given by the angle made by the length-wise side of the farm land with respect to the South direction, measured clockwise.

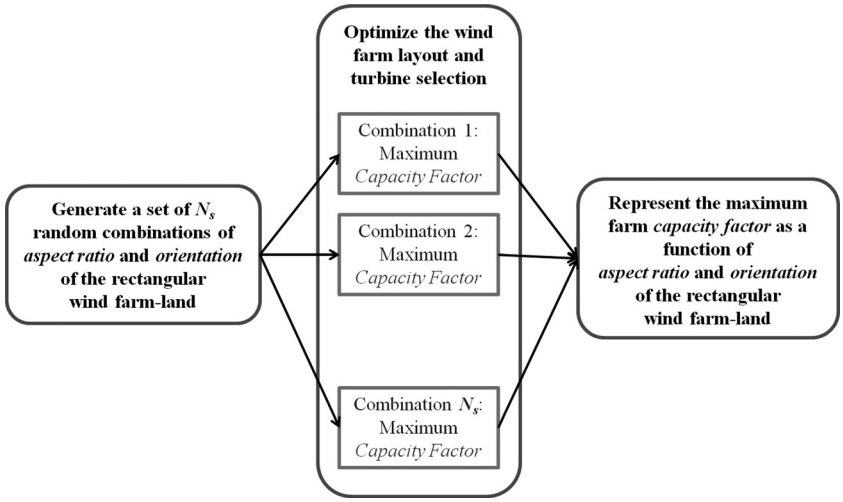

Fig. 2 Framework to model the relationship between the farm land configuration (*aspect ratio* and *orientation*) and the farm performance

In this paper, we have mainly considered a single contiguous rectangular land plot at the site. Although rectangular land plots are more popular, other land-shapes or sites with smaller disjointed plots also occur in practice. In such cases, the design framework developed in this paper could still be readily implemented on an approximated representation of the actual land-shape; this representation is accomplished by:

(1) Determining the smallest rectangle(s) that encloses the concerned shape or shapes (in case of disjointed land plots).
(2) Dividing the rectangle into a 2-D grid of an appropriate resolution.
(3) Restricting the placement of turbines to the grid cells that lie within the boundaries of the concerned shape (through additional constraints during optimization).

Gu and Wang [19] also presented an interesting method to model irregular farm land boundaries in the context of turbine micrositing. Their method is based on an edge detection algorithm that extracts wind farm contour information from existing digital maps.

The farm energy production potential or output potential in this paper is represented by the *capacity factor* (CF) of the farm. The farm CF is the ratio of (i) the actual energy expected to be produced over a given time-period to (ii) the energy that could have been produced if the farm would always be operating at its nameplate/installed capacity.

A design framework is formulated to model the relationship between the farm land-shape and the corresponding farm output potential; this framework comprises the following major steps:

(i) A set of sample *aspect ratios* and *orientations* are generated within specified practical ranges, using a pseudo-random sequence.
(ii) For each defined sample farm land-shape, the farm layout and the turbine selection are simultaneously optimized to maximize the CF of the farm (using the UWFLO method).
(iii) Using the information from the previous step (as training points), a response surface is fitted to represent the maximum CF as a function of the *aspect ratio* and the *orientation* of the rectangular farm land.

An illustration of this framework is provided in Fig. 2.

In the subsequent subsections, we provide a summary of the UWFLO energy production model, the formulation of the optimization problem for maximizing the CF, and the development of the "*land-shape to maximum CF*" response surface models.

2.2 UWFLO Energy Production Model. For a given incoming wind condition, the power generated by the entire wind farm, P_{farm}, is equal to the summation of the power generated by the individual turbines, which is expressed as

$$P_{\text{farm}} = \sum_{j=1}^{N} P_j \tag{1}$$

where P_j represents the power generated by Turbine-j, and N represents the number of turbines in the farm. For any given incoming wind speed and direction, the power generated by the individual turbines is determined by the UWFLO power generation model.

A brief summary of the steps in the UWFLO power generation is as follows:

(i) *Farm Layout*: A fixed X–Y co-ordinate system is defined such that the positive X-axis, which represents the lengthwise side of the farm, aligns with the South direction. The location of each turbine is defined in terms of this co-ordinate system. Transformed co-ordinates (x–y) are then determined for each turbine based on the wind direction.
(ii) *Wake Effects*: Based on the relative location of the turbines and the turbine features, it is determined which turbines are (fully/partially) in the wake of other turbines; a wake growth model is used for this purpose. Subsequently, analytical wake velocity-deficit formulations are used to determine the effective (rotor-averaged) speed of the wind in front of each turbine. In this case, the incoming wind speed profile can be characterized using either the log law [15] or the power law [14].
(iii) *Turbine Power Output*: The power output (P_j) from each turbine is determined from the estimated effective wind speed in front of it, using the power curve provided by the turbine-manufacturer.

It is helpful to note that the accuracy of the analytical power generation model is meaningfully sensitive to that of the standard analytical wake models used. The discussion of the inherent assumptions in the analytical wake model and the detailed description of the power generation model can be found in the papers by Chowdhury et al. [14,15].

Wind conditions at a site vary significantly with time. Hence, a reliable prediction of the expected annual energy production (AEP) of a wind farm should account for the *joint* variations of wind speed and wind direction at the site. To this end, the annual

distribution of wind speed and direction is first represented using a suitable probability density function. Subsequently, the AEP is determined by integrating the power generation function over the estimated annual wind distribution. Assuming the farm operates continuously throughout the year (all 365×24 h), the AEP of a wind farm in kWh (E_{farm}) can be expressed as

$$E_{\text{farm}} = (365 \times 24) \int_{0\,\text{deg}}^{360\,\text{deg}} \int_{0}^{U_{\max}} P_{\text{farm}}(U,\theta)\, p(U,\theta) dU d\theta \quad (2)$$

where $U_{\max}$ is the maximum recorded wind speed at that location; and $p(U,\theta)$ represents the probability of occurrence of wind conditions defined by speed U and direction θ. In Eq. (2), $P_{\text{farm}}(U,\theta)$ represents the power generated by the farm for an incoming wind of speed U and direction θ. Currently operating wind turbines experience 4% downtime on average [28]; such downtime can also be readily accounted for in the above expression, assuming the overall wind distribution is practically similar to that during the uptime hours.

The power generated by the group of turbines in a wind farm (P_{farm}) is a complex function of the incoming wind attributes, the arrangement of turbines, and the turbine features; it is not a tractable analytical function that can be directly integrated. Hence, a numerical integration approach [29] is suitable for estimating the AEP (defined in Eq. (2)). To this end, the Monte Carlo integration method is implemented using the Sobol's quasirandom sequence generator [30]. In this method, the AEP is evaluated as a summation over a set of the sample wind conditions. The approximated annual energy production is expressed as

$$E_{\text{farm}} = (365 \times 24) \sum_{i=1}^{n_p} P_{\text{farm}}\left(U^i,\theta^i\right) p\left(U^i,\theta^i\right) \Delta U \Delta\theta \quad (3)$$

where

$$\Delta U \Delta\theta = (U_{\max} \times 360\,\text{deg})/n_p$$

and where n_p is the number of sample points used; the parameters, U^i and θ^i, respectively, represent the speed and the direction of the ith sample incoming wind condition. For the case study in this paper, we consider the air density to be constant. The probability of wind speed and direction, $p\left(U^i,\theta^i\right)$, is estimated by the *Multivariate and Multimodal Wind Distribution* (MMWD) model [31,32]. The MMWD model, which uses a KDE-based joint distribution method, is uniquely capable of representing multimodally distributed wind data; this capability allows more accurate estimation of energy production (over a time period) than possible with typical parametric wind distribution models.

Based on the AEP given by Eq. (2), the capacity factor (CF) of the farm can be expressed as

$$\text{CF} = \frac{\text{AEP}}{(365 \times 24) \sum_{j=1}^{N} P_{\text{rj}}} \quad (4)$$

where P_{rj} is the rated power of the generic Turbine-j, and N represents the number of turbines in the farm.

2.3 Optimization Problem Definition. The objective of wind farm optimization here is to maximize the CF for a given farm land-shape. The variables in the optimization problem are the locations of each turbine (X_j, Y_j) and the type of turbine (T) to be used—a total of "$2N+1$" design variables for a N-turbine farm. The turbines are selected from a list of $T_{\max}$ commercially available turbine variants. In this framework, the nameplate capacity of the wind farm is fixed, and turbines of a specified rated power are allowed to be installed. Hence, the number of turbines to be installed (N) in the farm remains fixed. The optimization problem for the rectangular wind farm is defined as

$$\begin{gathered} \text{Max CF}(V) \\ \text{subject to} \\ g_1(V) \le 0 \\ g_2(V) \le 0 \\ V = \{X_1, X_2, \ldots\ldots, X_N, Y_1, Y_2, \ldots\ldots, Y_N, T\} \\ T \in \{1, 2, \ldots, T^{\max}\} \end{gathered} \quad (5)$$

where the capacity factor, CF, is estimated from Eq. (4), and T^{max} represents the number of turbine types in the pool of turbines available for selection.

The inequality constraint g_1 represents the minimum clearance required between any two turbines, and is given by

$$g_1(V) = \sum_{i=1}^{N} \sum_{\substack{j=1 \\ j \ne i}}^{N} \max\left(\left(0.5\left(D_i + D_j\right) + \triangle_{\min} - d_{ij}\right), 0\right) \quad (6)$$

where

$$d_{ij} = \sqrt{\Delta X_{ij}^2 + \Delta Y_{ij}^2}$$

In Eq. (6), D_i and D_j, respectively, represent the rotor-diameters of Turbine-i and Turbine-j, and $\triangle_{\min}$ is the minimum clearance required between the outer edge of the rotors of these two turbines. The parameters, ΔX_{ij} and ΔY_{ij}, represent distances between the locations of Turbine-i and Turbine-j along the X and Y axes, respectively. In this research, the value of the minimum spacing between turbines ($\triangle_{\min}$) is set at half of the mean rotor diameter of commercially available turbines. In practice, a greater minimum spacing might be necessary to mitigate the undesirable dynamic-loading effects induced by wake turbulence.

To ensure the placement of the wind turbines within the rectangular wind farm boundaries, the bounds for the generic X_i and Y_i variables are reformulated into the inequality constraint, g_2, which is given by

$$g_2(V) = \frac{1}{2N} \left(\begin{array}{l} \frac{1}{L} \sum_{i=1}^{N} \max(-X_i, X_i - L, 0) \\ + \frac{1}{B} \sum_{i=1}^{N} \max(-Y_i, Y_i - B, 0) \end{array} \right) \quad (7)$$

where the parameters L and B, respectively, represent the length and the breadth of the farm land.

2.4 Development of the Response Surface-Based Models. Response surfaces comprise a class of analytical approximation functions that are popularly used to represent complex functional relationships. Such approximation functions are generally necessary for real life design problems where relationships among important parameters are not analytically well defined and/or are expensive to evaluate. The dependence of the maximum CF (obtained through optimal turbine selection and placement) on the farm land-shape is not a straightforward analytical function. Secondly, it is computationally expensive to explore the maximum farm capacity factor for different values of land *aspect ratio* and *orientation*—an entire optimization process is required every time. Hence, we adopt the response surface methodology to model and investigate the relationship between the maximum capacity factor and the farm land-shape parameters.

First, a set of N_s sample land-shapes (aspect ratio and orientation values) are generated using Sobol's quasirandom sequence generator. The total land area of the farm is assumed to be fixed, and is represented by A_{farm}. For a sample farm land-shape, defined by the aspect ratio, a_R, and orientation, ϕ (in degrees), the dimensions of the rectangular farm can be expressed as

$$\begin{aligned} B &= \sqrt{A_{\text{farm}}/a_R} \\ L &= B \times a_R \end{aligned} \quad (8)$$

As the orientation (ϕ) of the rectangular farm land changes, the fixed X-axis is no more aligned with the South direction; instead it is now aligned at an angle ϕ with the South (measured clockwise). Therefore, the transformed co-ordinates of each turbine, in the power generation model, has to be reformulated as

$$\begin{bmatrix} x_i \\ y_i \end{bmatrix} = \begin{bmatrix} \cos\hat{\theta} & -\sin\hat{\theta} \\ \sin\hat{\theta} & \cos\hat{\theta} \end{bmatrix} \begin{bmatrix} X_i \\ Y_i \end{bmatrix} \quad \text{where} \quad \hat{\theta} = \begin{cases} \theta - \phi, & \text{if} \quad \theta > \phi \\ \theta - \phi + 360, & \text{otherwise} \end{cases} \tag{9}$$

where θ is the direction of wind in degrees, measured clockwise with respect to the South direction; the co-ordinates (X_i, Y_i) represent the location of turbine-i based on the fixed coordinate system, and (x_i, y_i) represent the transformed co-ordinates of that turbine with respect to a particular wind direction.

Each sample combination of *aspect ratio* and *orientation* of the farm land therefore translates into a unique combination of (i) farm land dimensions (boundaries), (L, B), and (ii) a modification to the transformed co-ordinates of the turbines within the farm power generation model. For each of these combinations, the UWFLO method is applied to optimize the *farm layout and turbine selection* with the objective of maximizing the CF of the farm—a total of N_s optimizations are thus performed. Using the maximum accomplished CF values from the N_s wind farm optimizations, response surfaces are trained to relate the *aspect ratio* and *orientation* of the farm land with the maximum CF.

Two surrogate modeling methodologies are used to represent the maximum capacity factor function: (i) the Quadratic Response Surface (QRS) method, and (ii) the Kriging Method. The QRS method is used to explore and understand the overall trend of maximum capacity factor variation under the impact of changes in the land-shape. The actual response is expected to be noisy, since the output is obtained through heuristic optimization (PSO); the likely level of uncertainty in the training data can lead to oscillations in the CF response function if a typical interpolating surrogate (e.g., radial basis functions and Kriging) is used. In contrast, the QRS can provide a smoother representation of the "*land-shape—maximum capacity factor*" relationship. The trained QRS also involves fewer parameters, thereby allowing more tractable exploration of the relationship and facilitating general guidance in land-shape decision-making. On the other hand, the Kriging surrogate is expected to provide a more accurate local representation of the "*land-shape—maximum capacity factor*" relationship, and is hence considered a more suitable choice for the process of optimizing the land-shape.

The generic quadratic response surface representing the "*land-shape—maximum capacity factor*" relationship can be expressed as

$$\mathrm{CF}_{\max}^{\mathrm{QRS}} = c_0 + c_1 a_{\mathrm{R}} + c_2\phi + c_3 a_{\mathrm{R}}^2 + c_4\phi^2 + c_5 a_{\mathrm{R}}\phi \tag{10}$$

where c_0, c_1, c_2, c_3, c_4, and c_5 are unknown coefficients that are determined by the least squares approach; and $\mathrm{CF}_{\max}$ represents the maximum capacity factor obtained through layout optimization. The training points to the response surface are obtained by optimizing the wind farm configuration (as in Eq. (15)) for the N_s parameterized sample farm land-shapes.

The Kriging surrogate model [33] for the "*land-shape—maximum capacity factor*" relationship can be expressed as

$$\mathrm{CF}_{\max}^{\mathrm{Krig}} = G(a_{\mathrm{R}}, \phi) + Z(a_{\mathrm{R}}, \mathrm{phi}) \tag{11}$$

where G is the known approximation (usually polynomial) function, and Z is the realization of a stochastic process with a zero mean and a nonzero covariance. The (i, j)th element of the covariance matrix of Z is given by

$$\mathrm{COV}[Z(a_{\mathrm{R}}^i, \phi^i), Z(a_{\mathrm{R}}^j, \phi^j)] = \sigma_Z^2 R_{ij} \tag{12}$$

where R_{ij} is the correlation between the ith and the jth training points; and σ_z^2 is the process variance. A Gaussian function is used as the correlation function. An efficient MATLAB implementation of the Kriging surrogate, developed by Lophaven et al. [34], is used in this paper. The order of the global polynomial trend function (G) is specified to be zero.

3 Illustrating the Role of Farm Land-Shape

3.1. Case Study: Description and Settings. A case study is performed for a site at the Baker wind station in North Dakota to illustrate the effectiveness of the proposed framework in modeling the influence of farm land-shape on the energy production potential of the site. The corresponding wind data are obtained from the North Dakota Agricultural Weather Network (NDAWN) [35]. To fit the wind distribution, we use the daily averaged data for wind speed and direction, measured at the Baker station between the years 2000 and 2009. Further details of the Baker station pertinent to this case study are provided in Table 1. The installed capacity and the total land area of the farm are specified to be 25 MW and 840,000 m^2, respectively, i.e., equivalent to a frugal *land area per MW installed* of 33,600 m^2/MW. In practice, land area of current wind farms in the US are generally above 120,000 m^2/MW installed [36]. We use a significantly smaller land area to explore if changing the land-shape could help extract more energy from tightly spaced turbine arrays, thereby alleviating high land footprint concerns regarding wind energy projects. In this case study, only 2.5 MW turbines are allowed to be installed, and a minimum inter-turbine clearance of 1.5 rotor diameters (between towers) is imposed (through Eq. (6)).

Geometrical redundancies exist in the combination of aspect ratio and orientation, depending on their considered ranges. In this context, it is helpful to note that

$$(a_{\mathrm{R}}, \theta) \equiv (a_{\mathrm{R}}, \theta + 180) \equiv \left(\frac{1}{a_{\mathrm{R}}}, \theta + 270\right) \tag{13}$$

In order to develop the response surface, a set of 50 sample values of *aspect ratio* and *orientation* are thus generated within the following specified ranges: $1 < a_{\mathrm{R}} < 10$ and $0\,\mathrm{deg} < \phi < 180\,\mathrm{deg}$. The upper limit of the aspect ratio would approximately allow a "*three rotor diameter*" spacing between the turbines when collinearly aligned.

3.2 Wind Farm Layout Optimization Results. A population of $20 \times (2N + 1)$ and a total number of 50,000 function evaluations (119 iterations) were allowed during wind farm optimization in this case study. Through numerical experiments, the allowed number of function calls was found to be sufficient for convergence with the MDPSO algorithm. Additional termination criteria inside MDPSO stops the optimization process when the relative change in the optimum value is less than 1×10^{-6} in 10 consecutive iterations. We use the same values of the user-defined

Table 1 Details of the weather station at Baker, ND [35]

Parameter	Value
Location	Baker, ND
Period of record	01/2001/2000 to 12/31/2009
Latitude	48.167 deg
Longitude	−99.648 deg
Elevation	512.0 m
Measurement height	3.0 m
Average roughness	0.1 m (grassland)
Average air density	1.2 kg/m^3

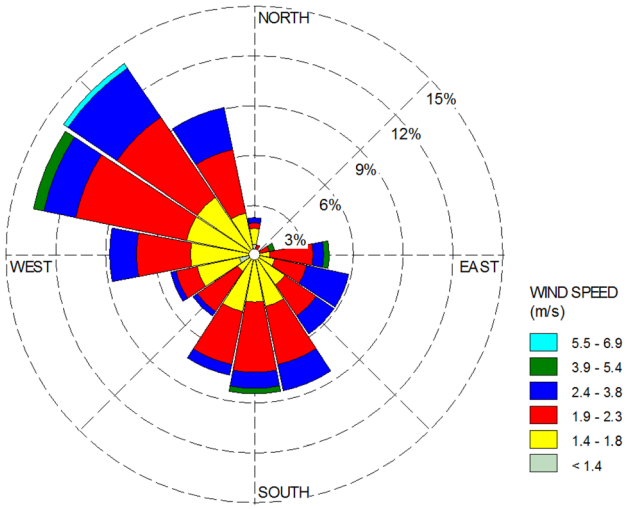

Fig. 3 Wind-rose diagram for the site at Baker [31]

parameters in mixed-discrete PSO as recommended and used by Chowdhury et al. [15]. The same 2.5 MW turbine with a 100 m rotor and a 100 m tower was optimally chosen for each sample farm land-shape. Different farm layout patterns were obtained for the different specified sample values of *aspect ratio* and *orientation*. This observation illustrates that the optimal layout pattern is strongly influenced by the specified/allowed land-shape.

The sample farm with an *aspect ratio* of 8.88 and a 157.5 deg orientation yielded the highest capacity factor ($CF_{max} = 0.658$), upon wind farm optimization. The sample farm with an *aspect ratio* of 1.28 and a 95.6 deg orientation yielded the lowest capacity factor ($CF_{max} = 0.629$), on wind farm optimization. The difference in the maximum capacity factor obtained for the best and the worst performing farm land-shapes is 4.6%—this difference approximately translates into a substantial revenue difference of \$10.5 million (at \$0.08/kWh COE) over a 20 year lifetime of the 25 MW project.

The optimized layouts for the best and the worst performing farm land-shapes are illustrated in Figs. 4(*a*) and 4(*b*), respectively. To explain the optimized layouts obtained and the CF response surfaces constructed in Sec. 3.3, the wind-rose diagram (Fig. 3) for the case-study site is shown below. In the wind-rose diagram, each of the sixteen sectors represents the respective probability of wind blowing from that direction.

A careful analysis of Figs. 4(*a*) and 4(*b*) show that land-shapes with higher aspect ratio allow turbines to be comparatively more spread out streamwise with respect to the dominant wind directions (shown in wind-rose diagram—Fig. 3). This allowance reduced the wake losses and promoted an increase in the capacity factor. In general, an ideal land-shape scenario would be a collinear alignment of wind turbines along a line that is perpendicular to a sharply dominant wind direction (if one exists); such an ideal scenario would allow negligible wake losses. Unfortunately, wind distributions in practice more often than not do not fit into the "*sharp dominant wind direction*" category, as evident from the current case study. As a result, a quantitative exploration (as presented here) of what type of land-shapes might provide greater energy production for a given wind pattern becomes all the more important even before considering the availability of land at the site in practice.

3.3 Capacity Factor Response Surface. The following quadratic response surface is obtained to represent the maximum CF as a function of the *aspect ratio* and *orientation* of the rectangular wind farm land

$$CF_{max}^{QRS} = 6.46 \times 10^{-1} + 1.73 \times 10^{-3} a_R - 3.60 \times 10^{-4}\phi - 3.21 \times 10^{-5} a_R^2 + 1.81 \times 10^{-6}\phi^2 + 3.98 \times 10^{-6} a_R \phi \quad (14)$$

The root mean squared error and the maximum absolute error of this QRS (Eq. (14)) were, respectively, estimated to be 0.45% and 1.08%, which can be considered to provide acceptable accuracy for the current application. The 3D plot and the contour plot of the QRS for CF_{max} are shown in Figs. 5(*a*) and 5(*b*), respectively.

For an aspect ratio of 1 (square shape), relatively smaller differences in maximized CF are expected with varying orientations, which is indeed observed in Figs. 5(*a*) and 5(*b*). Figures 5(*a*) and 5(*b*) show that the variation of CF is somewhat symmetric around the 90 deg orientation (East-West). Farm lands oriented East-West (90 deg) are observed to produce less energy than those oriented North-South (0 deg or 180 deg), which can be explained by the wind-rose diagram. The wind-rose diagram (Fig. 3) shows that winds from the West-North-West (WNW) and the South (S) are predominant at the Baker site. Under such a wind pattern, the smaller aspect ratios together with East-West orientation (e.g., the

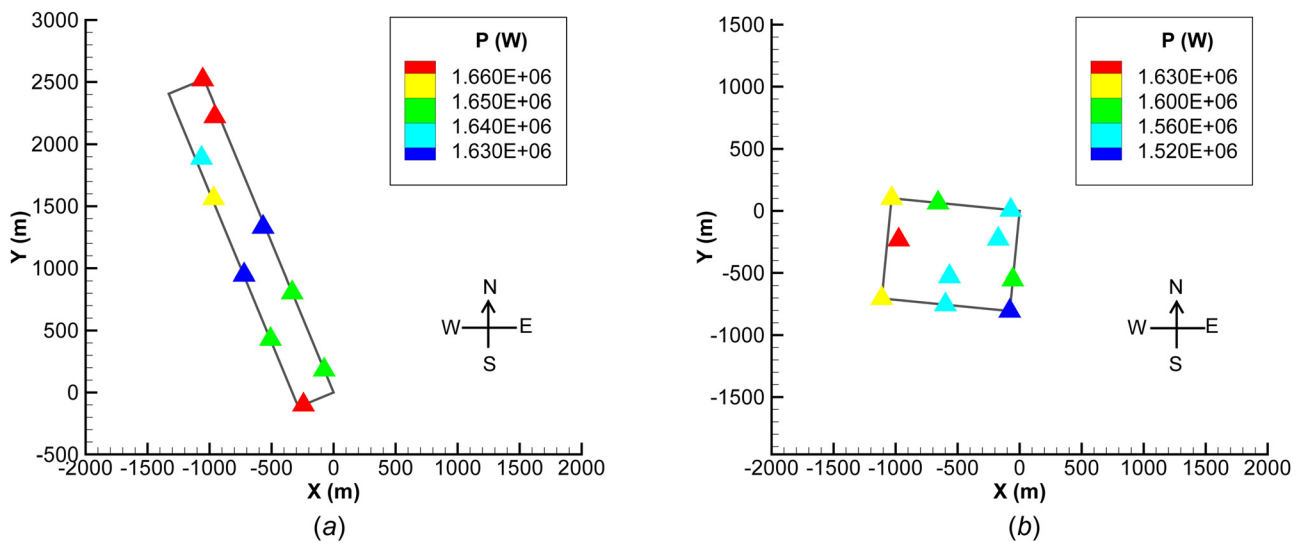

Fig. 4 Optimized farm layouts for sample farm land-shapes

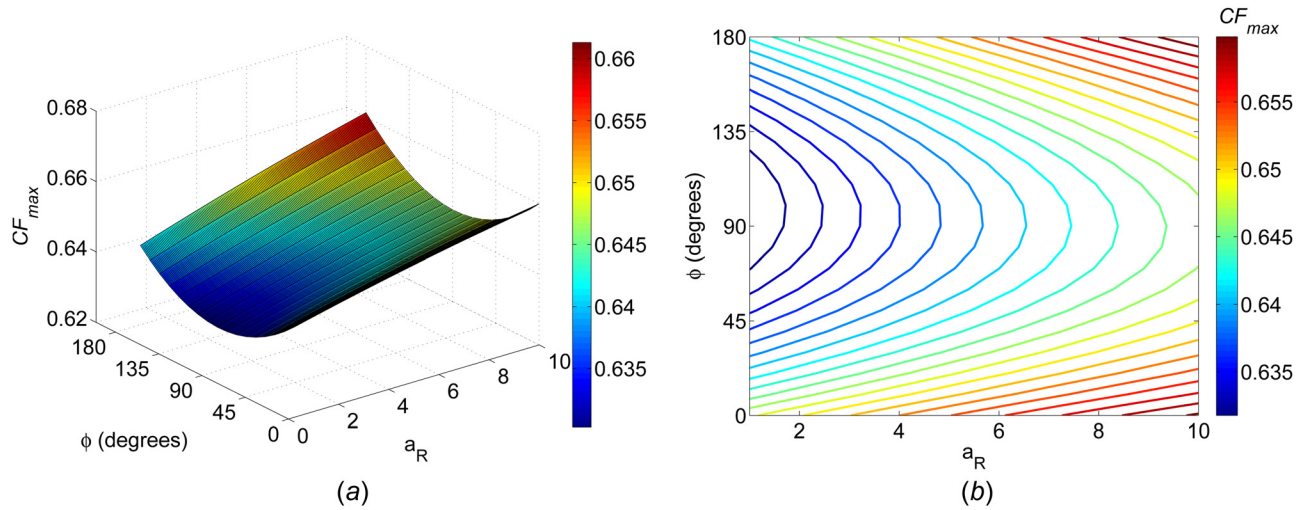

Fig. 5 Variation of the maximized farm capacity factor (CF_{max}) with respect to the farm land *aspect ratio* (a_R) and *orientation* (ϕ), as given by the quadratic response surface

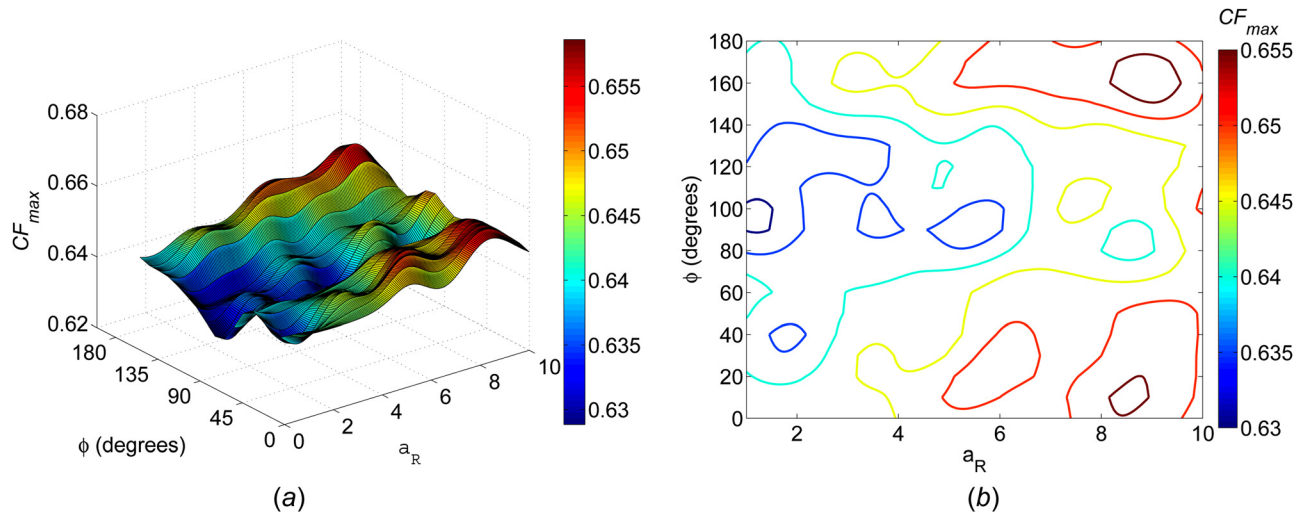

Fig. 6 Variation of the maximized farm capacity factor (CF_{max}) with respect to the farm land *aspect ratio* (a_R) and *orientation* (ϕ), as given by the Kriging surrogate model

layout in Fig. 4(*b*)) pack the turbines close to each other, streamwise, with respect to both dominant wind directions, leading to maximum wake losses.

For the given wind pattern (Fig. 3), the wind direction going across "*North of North-West and South of South-East (NNW-SSE)*" (both ways) is the effective *dominant wind direction axis*. Allowing greater distances between turbines along the *dominant wind direction* and staggered layout patterns in general minimize the wake losses, thereby increasing the CF. In this case, the dominant axis is slightly staggered (in angle) to the actual dominant wind directions (WNW and S). Hence, farm configurations with greater aspect ratios and aligned along (or close) to the dominant axis lengthwise are expected to extract more energy from this wind site. The illustrations in Figs. 5(*a*) and 5(*b*) agree with these hypotheses. The best performing farm land-shape (among the sample farm land-shapes) shown in Fig. 4(*a*) is likewise oriented along the effective *dominant wind direction axis*−22.5 deg West of North.

It is evident from the above illustrations that in the case of wind sites with multiple dominant wind directions (and/or skewed wind direction distributions), intuitive decision-making of suitable land-configurations becomes significantly challenging. This challenge necessitates a quantitative approach as presented in this paper.

The trained Kriging model yields a generalized least squares estimate of 0.097, and a maximum likelihood of the process variance of 4.04×10^{-05}. The 3D plot and the contour plot of the Kriging model for maximum CF are shown in Figs. 6(*a*) and 6(*b*), respectively. A similarity in the general trend captured by the QRS and Kriging surrogate can be observed, where:

(i) Farm lands with higher aspect ratios and a NNW-SSE orientation allow greater energy production potential.
(ii) Farm lands with smaller aspect ratios (close to one) and/or East–West orientation provide lower energy production potential.

However, owing to the inherent nature of interpolating surrogates, the Kriging CF function exhibits multiple modes (unlike the QRS), i.e., multiple local maxima of CF in the $a_R - \phi$ space. Land-shapes with aspect ratios between 8 and 9 and orientations of roughly 160 deg and 10 deg are observed to provide the most attractive energy production potential. These observations

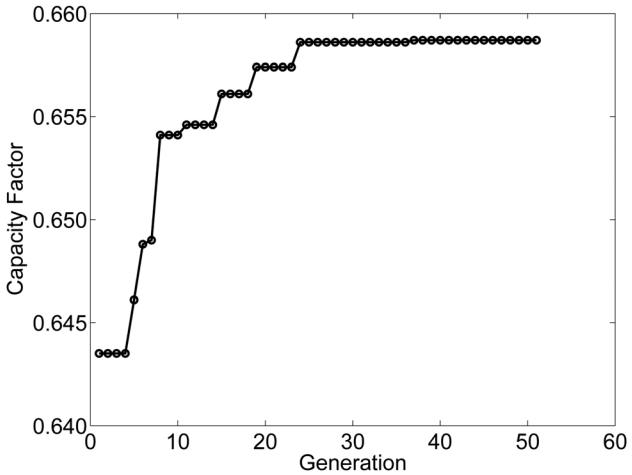

Fig. 7 Convergence history for optimizing the wind farm land-shape

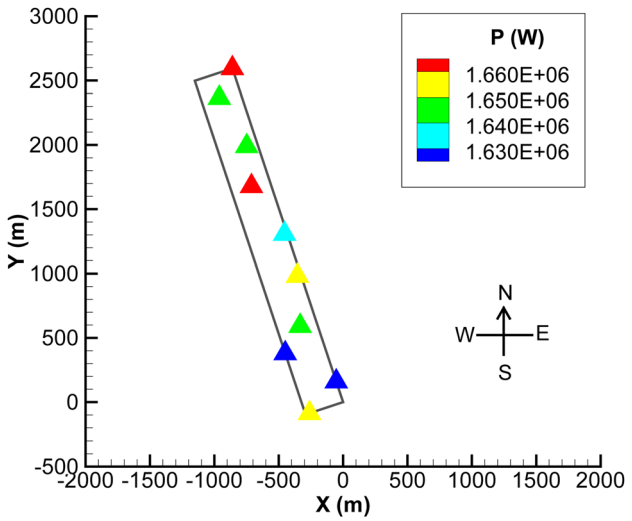

Fig. 8 Optimized farm layout corresponding to the optimum land-shape ($a_R = 8.9; \phi = 161.7$ deg)

encourage the optimization of the land-shape to investigate the maximum possible capacity factor obtainable from this site (for fixed land area and installed capacity).

3.4 Optimizing the Land-Shape. The land-shape is optimized with the objective to maximize the capacity factor. To this end, we use the Kriging surrogate relating the CF (obtained through layout optimization) to the land-shape. The land area is fixed at the same value as in the layout optimization (Sec. 3.1). The optimization problem is formulated as

$$\begin{aligned} &\text{Max} \quad \mathrm{CF}_{\max}^{\mathrm{Krig}}(a_R, \phi) \\ &\text{subject to} \\ &1 \le a_R \le 10 \text{ and } 0\,\text{deg} \le \phi \le 180\,\text{deg} \end{aligned} \tag{15}$$

where $\mathrm{CF}_{\max}^{\mathrm{Krig}}(a_R, \phi)$ is given by Eq. (11).

Since the optimization problem is relatively simple (i.e., unconstrained, continuous, and 2-dimensional), a standard genetic algorithm (MATLAB implementation) is applied to solve the optimization. A population size of 50, a crossover fraction of 0.8, and a termination tolerance of 1×10^{-6} on the fitness function value is used for this purpose. The optimization converged in 50 generations, with multiple runs yielding the same optimum within a *maximum objective function* tolerance of 1×10^{-4}. The convergence history of one of the representative runs is shown in Fig. 7. The capacity factor improved by approximately 2.3% during optimization, to reach a maximum value of $\mathrm{CF}_{\max} = 0.659$. This maximum CF represents a 4.8% improvement over the worst sample land-shape (Fig. 4(*b*)). The optimum aspect ratio and orientation were found to be 8.9 and 161.7 deg (18.3 deg West of North), respectively.

To validate the maximum CF estimated by the response surface, we perform layout optimization (using UWFLO) on the optimum land-shape ($a_R = 8.9; \phi = 161.7$ deg) yielded by the response surface. A maximum CF of 0.658 is obtained by layout optimization, which is a close match to that obtained from the response surface ($\mathrm{CF}_{\max} = 0.659$), thereby illustrating the robustness of the response surface in the context of land-shape design. The optimized wind farm layout obtained for this optimum land-shape is shown in Fig. 8. Since, this optimum land-shape is close to the best land-shape among the 50 samples (Fig. 4(*a*), the optimized turbine arrangements of the two land-shapes share certain characteristics. For example, both wind farm layouts (Figs. 4(*a*) and 8) contain two corner turbines, at the top-right and bottom-left corners.

4 Concluding Remarks

This paper developed a wind farm design framework that advances the understanding of how the optimum wind farm performance (or farm output potential) is influenced by the farm land-shape. The optimum planning of the farm layout (turbine arrangement) is not independent of the decisions made regarding the farm land-shape. The framework presented in this paper initiates important investigation into how these factors are interrelated in their collective influence on the overall energy production capacity of the farm. In this paper, the farm land-shape is parameterized in terms of the *aspect ratio* and the *orientation* of the rectangular farm land. A set of sample *aspect ratio* and the *orientation* values are first generated (assuming fixed farm land area), and the farm layout and turbine selection are optimized for each sample farm land-shape. The maximum CF thus obtained is represented as a function of the *aspect ratio* and the *orientation* using a quadratic response surface and a Kriging surrogate. The contour plots of the CF response functions provide important insights into the suitable choice of farm land-shapes for the specific case study, and incites an appreciation of such a (otherwise lacking) quantitative exploration of farm land-shapes.

The utility of this unique framework is illustrated through a case study performed for a site in North Dakota. We found that, higher CF could be accomplished for farm lands that have aspect ratios significantly greater than one and are oriented close to the *dominant wind direction axis*, where the latter is slightly staggered with respect to the actual dominant wind directions. Further investigation is however necessary to explore other wind distribution scenarios, e.g., sites with multiple prevalent wind directions that are perpendicular to each other. Overall, it is evident from the case study that, for practical wind resource variations, the complexity of the relationship between "*land-shape*" and "*wind farm output potential*" can far exceed the capabilities of intuitive decision-making. A generalized numerical/computational framework, as presented in this paper, is therefore necessary in effectively planning land configurations for wind energy projects. In this context, the exploration of land configurations other than contiguous rectangular plots would further establish the effectiveness of the proposed wind farm design methodology. Other important considerations in the context of land-shape planning include topography and soil quality variation at the site. Topography regulates the spatial variation of wind conditions, and the soil quality affects the feasibility/cost/type of turbine foundations to be used. These factors therefore comprise additional important topics for future research regarding the role of land-shape in wind farm layout planning.

Acknowledgment

Support from the National Science Foundation Awards CMMI 0946765 and CMMI 1100948 is gratefully acknowledged. Any opinions, findings, and conclusions or recommendations expressed in this paper are those of the authors and do not necessarily reflect the views of the NSF.

References

[1] Fronk, B. M., Neal, R., and Garimella, S., 2010, "Evolution of the Transition to a World Driven by Renewable Energy," ASME J. Energy Res. Technol., **132**(2), p. 021009.
[2] Prasad, B. J. S., 2010, "Energy Efficiency, Sources, and Sustainability," ASME J. Energy Res. Technol., **132**(2), p. 020301.
[3] Sorensen, P., and Nielsen, T., 2006, "Recalibrating wind turbine wake model parameters—validating the wake model performance for large offshore wind farms," European Wind Energy Conference and Exhibition, EWEA.
[4] Beyer, H. G., Lange, B., and Waldl, H. P., 1996, "Modelling Tools for Wind Farm Upgrading," European Union Wind Energy Conference, AIAA.
[5] Jensen, N. O., 1983, "A Note on Wind Turbine Interaction," Risoe National Laboratory, Roskilde, Denmark, Technical Report No. M-2411.
[6] Katic, I., Hojstrup, J., and Jensen, N. O., 1986, "A Simple Model for Cluster Efficiency," European Wind Energy Conference and Exhibition, EWEA.
[7] Frandsen, S., Barthelmie, R., Pryor, S., Rathmann, O., Larsen, S., Hojstrup, J., and Thogersen, M., 2006, "Analytical Modeling of Wind Speed Deficit in Large Offshore Wind Farms," Wind Energy, **9**(1–2), pp. 39–53.
[8] Larsen, G. C., Hojstrup, J., and Madsen, H. A., 1996, "Wind Fields in Wakes," EUWEC.
[9] Ishihara, T., Yamaguchi, A., and Fujino, Y., 2004, "Development of a New Wake Model Based on a Wind Tunnel Experiment," Global Wind, Technical Report, http://windeng.t.u-tokyo.ac.jp/ishihara/posters/2004_gwp_poster.pdf.
[10] Grady, S. A., Hussaini, M. Y., and Abdullah, M. M., 2005, "Placement of Wind Turbines Using Genetic Algorithms," Renewable Energy, **30**(2), pp. 259–270.
[11] Sisbot, S., Turgut, O., Tunc, M., and Camdali, U., 2009, "Optimal Positioning of Wind Turbines on Gokceada Using Multi-objective Genetic Algorithm," Wind Energy, **13**(4), pp. 297–306.
[12] Gonzalez, J. S., Rodriguezb, A. G. G., Morac, J. C., Santos, J. R., and Payan, M. B., 2010, "Optimization of Wind Farm Turbines Layout Using an Evolutive Algorithm," Renewable Energy, **35**(8), pp. 1671–1681.
[13] Kusiak, A., and Song, Z., 2010, "Design of Wind Farm Layout for Maximum Wind Energy Capture," Renewable Energy, **35**, pp. 685–694.
[14] Chowdhury, S., Zhang, J., Messac, A., and Castillo, L., 2012, "Unrestricted Wind Farm Layout Optimization (UWFLO): Investigating Key Factors Influencing the Maximum Power Generation," Renewable Energy, **38**(1), pp. 16–30.
[15] Chowdhury, S., Zhang, J., Messac, A., and Castillo, L., 2013, "Optimizing the Arrangement and the Selection of Turbines for a Wind Farm Subject to Varying Wind Conditions," Renewable Energy, **52**, pp. 273–282.
[16] Elia, S., Gasulla, M., and Francesco, A. D., 2012, "Optimization in Distributing Wind Generators on Different Places for Energy Demand Tracking," ASME J. Energy Res. Technol., **134**(4), pp. 041202.
[17] DuPont, B. L., and Cagan, J., 2012, "An Extended Pattern Search Approach to Wind Farm Layout Optimization," ASME J. Mech. Design, **134**(8), p. 081002.
[18] Mustakerov, I., and Borissova, D., 2010, "Wind Turbines Type and Number Choice Using Combinatorial Optimization," Renewable Energy, **35**(9), pp. 1887–1894.
[19] Gu, H., and Wang, J., 2013, "Irregular-Shape Wind Farm Micro-Siting Optimization," Energy, **57**, pp. 535–544.
[20] Chowdhury, S., Messac, A., Zhang, J., Castillo, L., and Lebron, J., 2010, "Optimizing the Unrestricted Placement of Turbines of Differing Rotor Diameters in a Wind Farm for Maximum Power Generation," ASME 2010 International Design Engineering Technical Conferences (IDETC), No. DETC2010-29129, ASME.
[21] Chowdhury, S., Tong, W., Messac, A., and Zhang, J., 2013, "A Mixed-Discrete Particle Swarm Optimization With Explicit Diversity-Preservation," Struct. Multidisciplinary Optimization, **47**(3), pp. 367–388.
[22] Chen, L., and MacDonald, E., 2012, "Considering Landowner Participation in Wind Farm Layout Optimization," ASME J. Mech. Design, **134**(8), p. 084506.
[23] Sahin, A. D., Dincer, I., and Rosen, M. A., 2006, "New Spatio-Temporal Wind Exergy Maps," ASME J. Energy Res. Technol., **128**(3), pp. 194–202.
[24] Kuvlesky, W. P., Brennan, L. A., Morrison, M. L., Boydston, K. K., Ballard, B. M., and Bryant, F. C., 2010, "Wind Energy Development and Wildlife Conservation: Challenges and Opportunities," J. Wildlife Manag., **71**(8), pp. 2487–2498.
[25] Windustry, 2010, "Landowner Guide: Evaluating a Wind Energy Development Company," Minneapolis, MN, http://www.windustry.org/sites/windustry.org/files/Landowner%20Guide%20to%20Evaluating%20a%20Developer.pdf.
[26] Christie, D., and Bradley, M., 2012, "Optimizing Land Use for Wind Farms," Energy Sustainable Dev., **16**(4), pp. 471–475.
[27] Chowdhury, S., Zhang, J., Messac, A., and Castillo, L., 2012, "Characterizing the Influence of Land Area and Nameplate Capacity on the Optimal Wind Farm Performance," ASME 2012 6th International Conference on Energy Sustainability, No. ESFuelCell2012-91063, ASME.
[28] Graves, A., Harman, K., Wilkinson, M., and Walker, R., 2008, "Understanding Availability Trends of Operating Wind Farms," AWEA Wind Power Conference, AWEA.
[29] Kusiak, A., and Zheng, H., 2010, "Optimization of Wind Turbine Energy and Power Factor With an Evolutionary Computation Algorithm," Energy, **35**, pp. 1324–1332.
[30] Sobol, M., 1976, "Uniformly Distributed Sequences With an Additional Uniform Property," USSR Comput. Math. Math. Phys., **16**, pp. 236–242.
[31] Zhang, J., Chowdhury, S., Messac, A., and Castillo, L., 2011, "Multivariate and Multimodal Wind Distribution Model Based on Kernel Density Estimation," ASME 2011 5th International Conference on Energy Sustainability, ASME.
[32] Zhang, J., Chowdhury, S., Messac, A., and Castillo, L., 2013, "A Multivariate and Multimodal Wind Distribution Model," Renewable Energy, **51**, pp. 436–447.
[33] Cressie, N., 1993, *Statistics for Spatial Data*, Wiley, New York.
[34] Lophaven, S., Nielsen, H., and Sondergaard, J., 2002, "Dace—A MATLAB Kriging Toolbox, Version 2.0," Technical University of Denmark, Informatics and Mathematical Modelling Report No. IMM-REP-2002-12.
[35] NDSU, "North Dakota Agricultural Weather Network," http://ndawn.ndsu.nodak.edu/, accessed, December 2010.
[36] Denholm, P., Hand, M., Jackson, M., and Ong, S., 2009, "Land-Use Requirements of Modern Wind Power Plants in the United States," Technical Report No. NREL/TP-6A2-45834, NREL.